PAPER AAS 95-351

ATTITUDE AND ORBIT DETERMINATION OF A TETHERED SATELLITE SYSTEM

Kyle T. Alfriend
Naval Postgraduate School

William J. Barnds
Swales & Associates, Inc.

Shannon L. Coffey
Naval Research Laboratory

Lynda M. Stuhrenberg
Appalachian State University

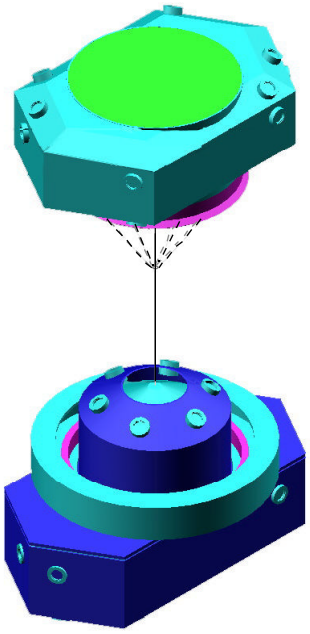

AAS/AIAA Astrodynamics Specialist Conference

HALIFAX, NOVA SCOTIA, CANADA **14-17 AUGUST 1995**

AAS Publications Office, P.O. Box 28130, San Diego, CA 92198

AAS 95-351

Attitude and Orbit Determination of a Tethered Satellite System

K. T. Alfriend[1]
W. J. Barnds[2]
S. L. Coffey[3]
L. M. Stuhrenberg[4]

Abstract

The Naval Research Laboratory is planning to launch a tethered satellite system (TiPS) in 1996. The system will consist of two small satellites connected by a 4 km tether. The purpose of the system is to study the dynamics and survivability of tether systems. There will be no attitude control system. Each of the subsatellites will have laser retroreflectors for laser tracking. In addition, at the center of mass (CM) of the system, there will be a half wavelength dipole to enhance radar tracking of the CM. The radar cross section (RCS) of the dipole will be approximately equal to the RCS of each of the subsatellites. Since the RCS of the dipole is highly sensitive to the aspect angle, and since it is likely that the tether system will be librating, tracking of the dipole may be difficult. Consequently, the orbit determination will not depend on tracking of the dipole.

In this paper the equations for the orbit and attitude determination of the system are developed and the results of simulations of the expected accuracy are presented. By attitude determination we mean attitude of the tether system, not attitude of each of the subsatellites. The tether system is modeled as an extensible, massless tether with longitudinal damping. The state consists of the epoch values of the CM position and velocity and the position and velocity of the tether end mass relative to the CM. Batch least squares is used to estimate the state. The state and variational equations are numerically integrated. Simplifications of the equations of motion result in two harmonic oscillator equations with different frequencies. Some analysis was performed to understand the impact of the simplifications on the orbit determination.

1 Introduction

The Naval Research Laboratory is building an experiment to study the physics of space tethered systems and to understand the survivability of tethers in the current debris-strewn space environment. The experiment is named TiPS (Tether Physics and Survivability Experiment). In general the orbit dynamics of a spacecraft must be inferred from processing ground observations. For a tethered system the process is complicated by many factors: the potentially large distances of the observed end masses relative to the CM, the pendulum motion of the tethered system, the quality, quantity and frequency of the observations, the nonstandard orbital motion of the observed end masses, the flexibility of the tether, and other perturbations specific to tethered systems. From the experiment, data on the observed positions of the end masses will be archived for future study of

[1]Navy TENCAP Chair, Space Systems Academic Group, Naval Postgraduate School, Monterey, CA 93943
[2]Aerospace Engineer, Swales & Associates Inc., Beltsville, MD 20705
[3]Head, Mathematics and Orbit Dynamics Section, Naval Research Laboratory, Washington, DC 20375
[4]Student, Appalachian State University, Boone, North Carolina, 28608

tether dynamics. To achieve the physics goal, we must be able to predict the motion of the end masses with sufficient accuracy for ground based satellite laser ranging facilities (SLR) to acquire and track the end masses. This paper describes the algorithms and software developed to provide for acquisition by SLR sites.

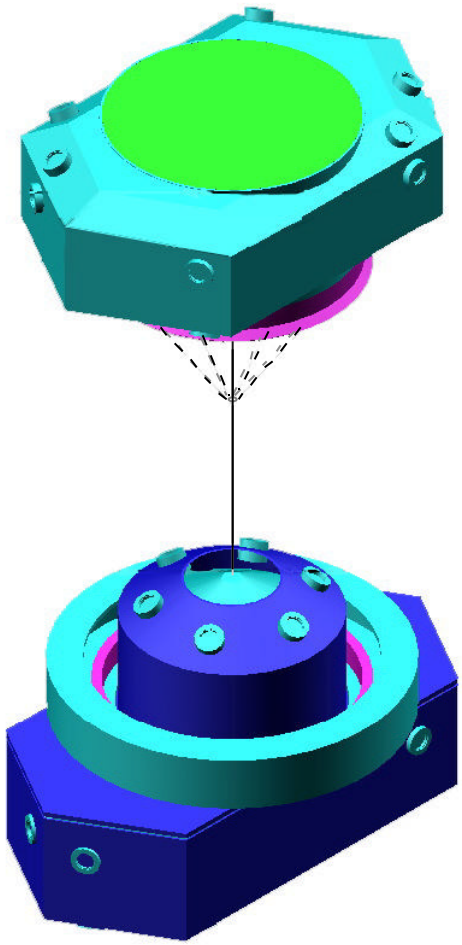

Figure 1: Tips Experiment in Deployed Configuration

The experiment (see Fig. 1) is being designed as a low cost secondary experiment piggy-backed on a DoD satellite. Telemetry downlink from the satellite will be established for only a very brief period when the tether is being deployed. Otherwise, the system will be completely passive. The dynamics of the system as well as knowledge of the survival of the tether will be derived from laser ranging data provided by ground based SLR sites. Tracking with lasers will provide high quality range as well as azimuth and elevation data.

Radar tracking will also be provided by the Air Force and Naval Space Commands. Either subsatellite or the dipole placed at the CM may be tracked. These data will then be processed in the normal fashion to provide two line element sets. Two problems exist. The two subsatellites are not in Keplerian orbits and the tracking data may consist of data on both subsatellites and the dipole. The result will be at best a gross estimate of the position of the center of mass. Thus, the data provided by the Space Surveillance system will not be sufficient for tracking the TiPS end masses. Typically a ground based laser has a beamwidth of 100-200 meters at the altitude of TiPS.

The normal solutions of radar "skin tracking" cannot meet this level of accuracy. The acquisition problem for TiPS is more difficult because of the length of the tether and the oscillatory motion of the end masses. For this reason it is necessary to estimate the parameters of the oscillatory motion. Initially it is expected that laser acquisition will have to be enhanced by telescope assistance, which is available at some SLR sites. Since telescopes require terminator lighting conditions it is expected that initial SLR data will be somewhat spotty. Eventually it is expected that sufficient data will be available to estimate the initial conditions of the end masses. Once good initial conditions for the tether state are produced, they will be provided to the SLR sites for predicting the motion of TiPS. This will enable the SLR sites to track TiPS whenever it is above the tracking horizon, given good weather conditions.

NASA's Goddard Space Flight Center will facilitate the tracking of the end masses by coordinating activities with the SLR sites, developing and installing tether specific software, and passing data and Extended Inter-Range Vectors (EIRV) between the SLR sites and NRL. An EIRV is an Inter-Range Vector augmented with parameters for the dynamics of the end masses. Tracking data from NASA as well as international SLR sites will be transmitted electronically to Goddard using communication facilities set up for retroreflector equipped satellites like Topex. From there NRL will receive the data by Internet and will process it into EIRVs. The EIRVs will then be sent electronically to Goddard for distribution to the SLR sites. It is expected that the normal updating will take about 1-2 hours in duration.

For the orbital motion of the TiPS system, we will consider all the mass as if it is concentrated at the center of mass instead of the center of gravity of the system. The reason we do not use the center of gravity is because there is little difference between the two for TiPS and the center of gravity changes for different orientations of the tether, which would complicate the mathematics needlessly.

2 System Description

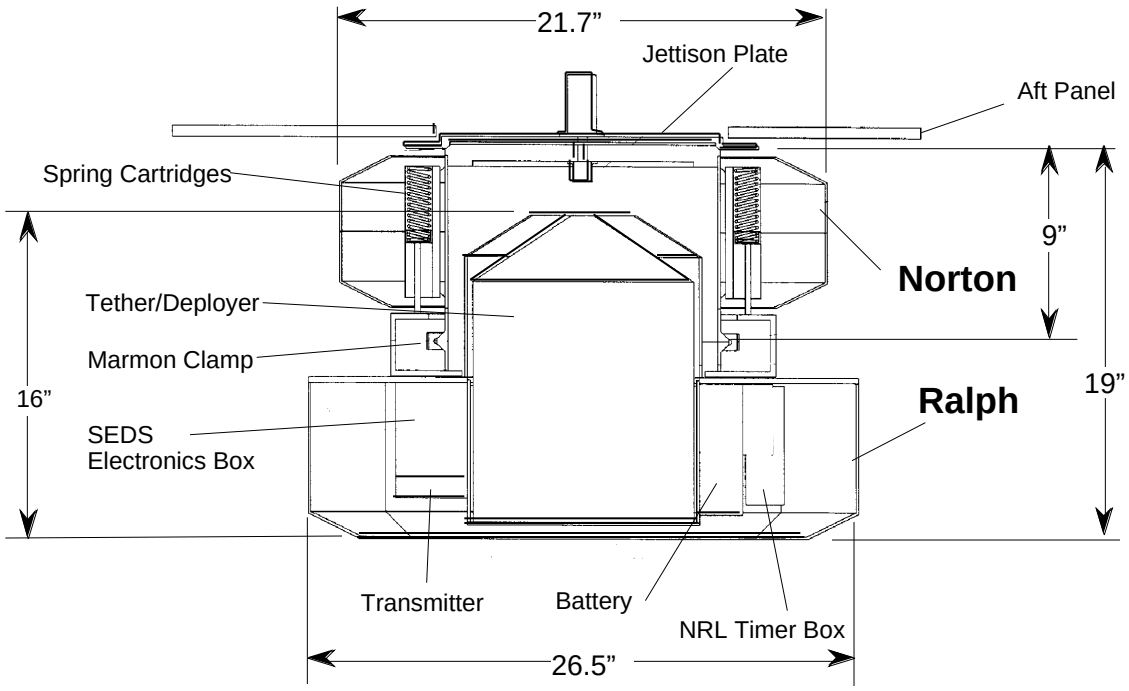

Figure 2: TiPS Assembly with Skin in Place

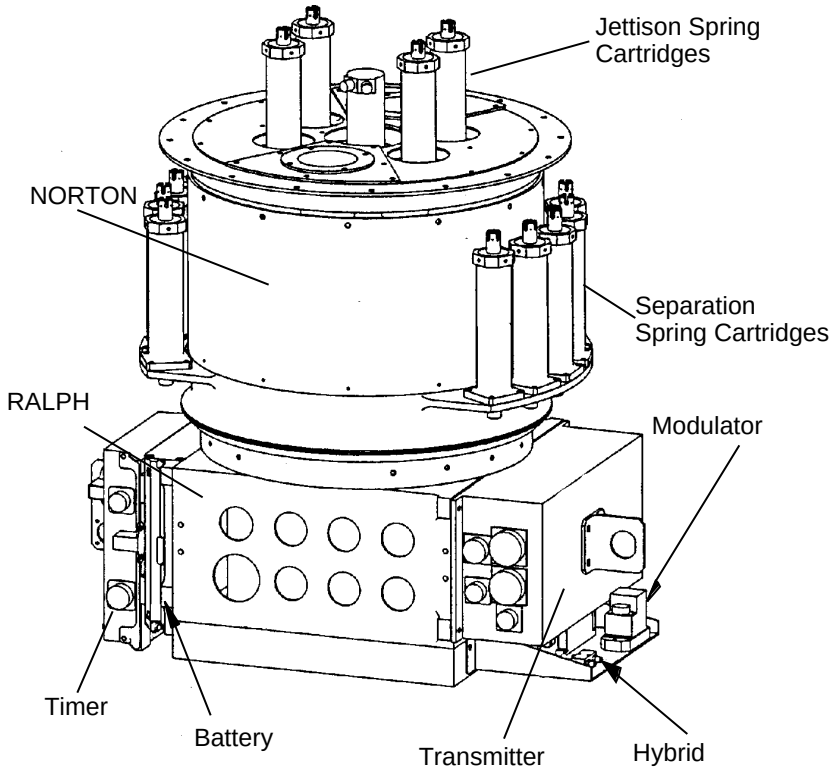

Figure 3: TiPS Assembly with Skin and Blankets Removed

The fully deployed TiPS payload consists of two bodies, Ralph and Norton, connected by a four kilometer tether. The aft panel shown in Figure 2 is attached to the host vehicle. The only electronics on the experiment is the SEDS[3] box provided by NASA which will count the number of turns of the tether as it is deployed, providing information on the rate of deployment. The SEDS box is located on Ralph. Norton does not contain any electronics. The timer is set to initiate separation between Ralph and Norton. The separation of Ralph from Norton is expected to take about 30 minutes. The rate at which the tether unspools will be broadcast repeatedly to the ground for as long as the battery holds out, approximately 8 hours. After this time TiPS will become a passive satellite. Ralph weighs approximately 95.3 lbs, Norton 22.4 lbs, and the tether about 12 lbs.

The tether for TiPS is made of Spectra-1000 which is 2-3 mm in diameter. Woven in the center of the tether is a yarn to make the tether puff up to increase its survivability.

3 Operations

TiPS is a self contained payload which will be jettisoned from a spinning host spacecraft. The jettison will be effected by four springs which will provide approximately 3 feet per second delta-v. Jettison attitude will be along the velocity vector. Upon jettison, the TiPS separation timer will be initiated. The separation between Ralph and Norton will occur approximately 1.66 revolutions after

jettison at a rate of approximately 16 ft/sec. At this time TiPS will be pointing ahead of nadir at an angle of approximately 31^o. The exact time of separation was determined by analysis to produce maximum gravity gradient pull to insure the deployment does not "stall." Both sets of springs can be seen in Figure 3.

The initial orbit for TiPS will be circular somewhere between 450 and 550 nm at an inclination of about 63.4^o. The final altitude will be selected to balance the requirement for long term survivability data and the desire to cleanse space of TiPS once its mission is over. Due to the cross sectional area of the tether, it will experience considerably more drag than a normal satellite of its mass and size. At the high end of the altitude range, the system would easily survive one complete solar cycle, but would reenter in about 4-5 years at the low end of the altitude range. The exact altitude had not been determined at the time of this report.

There are 18 retroreflectors mounted on both Ralph and Norton. Each retroreflector is one inch in diameter made of fused silica with a highly reflective silver coating on the back surface. The retroreflectors mounted on Norton are uncoated while those mounted on Ralph are coated with TiO_2 and SiO_2. Thus both end-bodies will reflect green (532nm) while those on Ralph do not reflect infrared (1064nm). The design allows unique identification of each end-body by those SLR sites equipped with dual wavelength lasers. This will provide data to resolve anomalies such as tether inversion.

As a consequence of the jettison orientation, it is expected that Ralph will be the bottom vehicle and Norton the top.

4 Mathematics of Tether Orbit Determination

In this section we will provide an outline of the mathematics of the orbit determination process. We will do so in a manner we hope is understandable without being too tedious in detail.

First let us discuss the general problem. The motion of an object is governed by a system of differential equations. We frequently refer to the state vector as the solution to this system. To predict the future state of the system we need to provide the initial conditions for the state vector. The prediction can be accomplished by either integrating numerically the differential equations or by applying an analytic solution, if such a solution exists, to the initial state vector. Since a particular vector of initial conditions determines the solution to the differential conditions we need to determine the initial conditions that best approximate the motion of the object of interest. The orbit determination problem is to find the initial conditions which minimize the difference between the estimated state and the observations. Assuming the environment does not change too radically we can then use that estimated initial condition state vector to predict the future state of the system.

In general the differential equations for a system are nonlinear and coupled. In the past it was necessary to simplify the equations so that computers could produce solutions in reasonable time. However, simplifications mean substituting an approximation for the original system. This can severely limit the model of the system, often to the extent that the solution does a poor job of predicting the motion of the system. With the advent of fast and relatively cheap computers, we now can discard the simplified system in favor of the full system. However, working with a decoupled linear set of equations does provide some insight into the local behavior of the full system and for this reason it is often valuable to build the simplified system as a sanity check on the full system. We have developed both for this problem and will compare them.

For our purpose we developed a batch least squares system for processing observations. Many variations of this approach exist, we chose ours to be compatible with the existing software used to process SLR data for normal satellites.

4.1 Least Squares Estimation

To differentially correct the initial conditions for an object, one must also have the partial derivatives of the state vector with respect to the initial conditions.

Let us briefly become tutorial and review the least squares algorithm. Suppose $\mathcal{O}(t)$ is an observation at some time t. Let $\mathbf{X}(t, \mathbf{Y})$ represent the state vector, $\mathbf{Y}$ represent the desired initial conditions for the state vector and $\mathbf{Y}_0$ an estimate of the initial conditions for the state vector. Recall the state vector is a function of time and the initial conditions. Then we form the cost function

$$\begin{aligned} J(\mathbf{Y}) &= [\mathcal{O}(t) - \mathbf{X}(t, \mathbf{Y})]^T W [\mathcal{O}(t) - \mathbf{X}(t, \mathbf{Y})] \\ &= [\mathcal{O}(t) - \mathbf{X}(t, \mathbf{Y}_0) - A(\mathbf{Y} - \mathbf{Y}_0)]^T W [\mathcal{O}(t) - \mathbf{X}(t, \mathbf{Y}_0) - A(\mathbf{Y} - \mathbf{Y}_0)], \end{aligned}$$

where $A = D_Y \mathbf{X}(t, \mathbf{Y}_0)$, and W is a weight matrix for the observations. This is the least squares equation. We seek to find a value for $\mathbf{Y}$ which minimizes the difference between the observation and the prediction of the function. Setting $J'(\mathbf{Y}) = 0$ we get

$$\mathbf{Y} = \mathbf{Y}_0 + (A^T W A)^{-1} A^T W (\mathcal{O}(t) - \mathbf{X}(t, \mathbf{Y}_0)), \tag{1}$$

which is the equation for updating the initial conditions. Given an initial estimate, $\mathbf{Y}_0$, for the initial conditions one successively iterates using equation (1) until the residuals $\mathcal{O}(t) - \mathbf{X}(t, \mathbf{Y}_0)$ become sufficiently small.

In reality, we will have a large set of observations to process. In this case we merely extend $\mathcal{O}$ to be a vector of observations, $\mathbf{X}(t, \mathbf{Y}_0)$ to be a vector of state vectors, and A to be a vector of matrices. Each block in $\mathbf{X}$ and A is evaluated at the time of the corresponding observation.

Thus we need to compute the state vector for the system as well as the partial derivative of the state vector with respect to the initial conditions.

4.2 Orbital Equations of Motion

A tethered system in orbit experiences two distinctly different motions. There is the orbital motion of the system which is the orbit of the center of mass about the earth, and a librational motion of the end bodies relative to the center of mass. Because of the two different types of motion, we build our orbit determination system by augmenting a standard orbit determination system with equations for the end bodies. For the center of mass we choose our coordinate frame fixed in the earth and centered at the earth's center. For the tether system we choose a coordinate frame rotating with the center of mass of the system, a so called local vertical, local horizontal (LVLH) system (see Figure 4).

Suppose $\mathbf{X}$ is the solution of the 12 dimensional first order system of equations,

$$\dot{\mathbf{X}} = \mathbf{F}(\mathbf{X}). \tag{2}$$

The first six of these equations are the usual equations for the center of mass and the last six represent the motion of the end mass relative to the center of mass. If we let $\mathbf{F} = col(\mathbf{F}_{CM}, \mathbf{F}_T)$, $\mathbf{X} = col(\mathbf{X}_{CM}, \mathbf{X}_T)$ and $\mathbf{X}_0 = col(\mathbf{X}_{CM0}, \mathbf{X}_{T0})$, then the initial value problem for the tether system looks like

$$\frac{d}{dt}\begin{pmatrix} \mathbf{X}_{CM} \\ \mathbf{X}_T \end{pmatrix} = \begin{pmatrix} \mathbf{F}_{CM}(\mathbf{X}_{CM}) \\ \mathbf{F}_T(\mathbf{X}_{CM}, \mathbf{X}_T) \end{pmatrix}, \quad \begin{pmatrix} \mathbf{X}_{CM} \\ \mathbf{X}_T \end{pmatrix}_{|t=t_0} = \begin{pmatrix} \mathbf{X}_{CM0} \\ \mathbf{X}_{T0} \end{pmatrix},$$

where $\mathbf{F}_{CM}$ is the right hand side of the orbit equations for the center of mass, and $\mathbf{F}_T$ is the right hand side of the differential equations for the tether. The tether equations will be discussed in Section 4.4.

Although the function $\mathbf{F}_{CM}$ will not depend on the tether dynamics, the tether equations will depend on the motion of the CM. Differentiating Eq. (2) with respect to the initial conditions we get

$$\frac{d}{dt}\frac{\partial \mathbf{X}}{\partial(\mathbf{X}_{CM0}, \mathbf{X}_{T0})} = \frac{\partial \mathbf{F}}{\partial \mathbf{X}}\frac{\partial \mathbf{X}}{\partial(\mathbf{X}_{CM0}, \mathbf{X}_{T0})}. \tag{3}$$

In component form we get

$$\frac{d}{dt}\begin{pmatrix} \dfrac{\partial \mathbf{X}_{CM}}{\partial \mathbf{X}_{CM0}} \\ \dfrac{\partial \mathbf{X}_T}{\partial(\mathbf{X}_{CM0}, \mathbf{X}_{T0})} \end{pmatrix} = \begin{pmatrix} \dfrac{\partial \mathbf{F}_{CM}}{\partial \mathbf{X}_{CM}} & 0 \\ \dfrac{\partial \mathbf{F}_T}{\partial \mathbf{X}_{CM}} & \dfrac{\partial \mathbf{F}_T}{\partial \mathbf{X}_T} \end{pmatrix} \begin{pmatrix} \dfrac{\partial \mathbf{X}_{CM}}{\partial \mathbf{X}_{CM0}} \\ \dfrac{\partial \mathbf{X}_T}{\partial(\mathbf{X}_{CM0}, \mathbf{X}_{T0})} \end{pmatrix}. \tag{4}$$

We will designate $\hat{A}$ as the derivative of the state vector with respect to initial conditions,

$$\hat{A} = \begin{pmatrix} \dfrac{\partial \mathbf{X}_{CM}}{\partial \mathbf{X}_{CM0}} \\ \dfrac{\partial \mathbf{X}_T}{\partial(\mathbf{X}_{CM0}, \mathbf{X}_{T0})} \end{pmatrix}.$$

The partial derivative function $\hat{A}$ is then constructed by integrating the variational Eq. (4) for the initial conditions

$$\hat{A}|_{t=t_0} = I.$$

Thus there will be the 12 Eq. (2) and a matrix (12 x 12) for the variational Eq. (4) to be integrated. To form the variational equations we must determine the entries $\partial \mathbf{F}/\partial \mathbf{X}$. These terms will be discussed in Section 4.6.

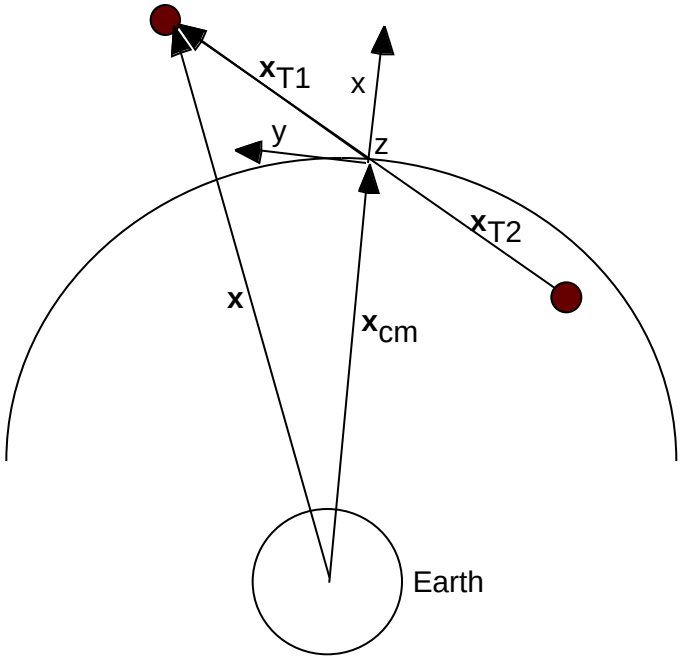

Figure 4: Coordinate Frames

4.3 Relating Observations to the State Vector

The coordinates of an end body are obtained from

$$\mathbf{x} = \mathbf{x}_{cm} + R\mathbf{x}_{Ti},$$

where R is the rotation of the LVLH coordinate frame to the inertial frame, and $\mathbf{x}_{Ti}, i = 1, 2$ represent Norton or Ralph respectively. Let the state vector for the center of mass of the tether system be denoted by

$$\mathbf{X}_{cm} = \text{col}(\mathbf{x}_{cm}, \mathbf{v}_{cm}),$$

where $\mathbf{x}_{cm}$ is the position vector for the center of mass, and $\mathbf{v}_{cm}$ is the velocity vector for the center of mass. The vector of initial conditions for the center of mass is

$$\mathbf{X}_{cm0} = \text{col}(\mathbf{x}_{cm0}, \mathbf{v}_{cm0}).$$

The state for the tether system is defined by

$$\mathbf{X}_T = \text{col}(\mathbf{x}_T, \mathbf{v}_T),$$

where $\mathbf{x}_T$ is the Cartesian vector to the end body, and $\mathbf{v}_T$ is the Cartesian velocity vector for that body. $\mathbf{X}_T$ is understood to be in the frame of reference rotating with the center of mass of the system. We now define this rotating coordinate frame. The x axis in $\mathbf{x}_T$ is radially outward, z is orbit normal, and y is approximately along the velocity vector.

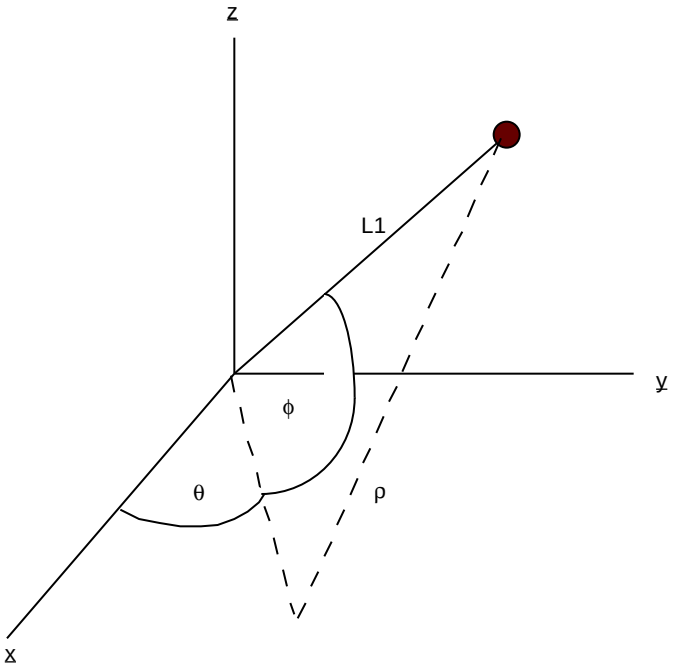

Figure 5: Spherical Coordinates

We will refer to $\mathbf{X}_{T0}$ as the vector of initial conditions for the tether state vector. For now we need not be concerned with whether we are in Cartesian or spherical coordinates.

Suppose f is a function of the state vector $\mathbf{X}$. For example f might be the transformation from earth fixed inertial coordinates to station fixed azimuth, elevation, and range coordinates. Then the partial derivative with respect to the initial conditions would be

$$\begin{aligned}
\frac{\partial f}{\partial \mathbf{X}_0} &= \left(\frac{\partial f}{\partial \mathbf{X}_{cm0}}, \quad \frac{\partial f}{\partial \mathbf{X}_{T0}} \right) \\
&= \left(\frac{\partial f}{\partial \mathbf{X}_{cm}} \frac{\partial \mathbf{X}_{cm}}{\partial \mathbf{X}_{cm0}} + \frac{\partial f}{\partial \mathbf{X}_T} \frac{\partial \mathbf{X}_T}{\partial \mathbf{X}_{cm0}}, \frac{\partial f}{\partial \mathbf{X}_T} \frac{\partial \mathbf{X}_T}{\partial \mathbf{X}_{T0}} \right).
\end{aligned}$$

Here we have made an assumption that the tether motion depends on the center of mass, but that the center of mass motion about the earth does not depend on the tether end masses. While not strictly true, the effect of the librational motion of the tether on the orbital motion is much smaller than neglected forces and can be safely, and thank goodness, ignored.

The state vector $\mathbf{X}$ is constructed by integrating numerically the differential equations for each component. In the case of the center of mass, $\mathbf{X}_{cm}$ represents the state vector for the center of mass. We provide in the next section the tether differential equations.

4.4 Tether Differential Equations

The tether system is modeled as two end masses connected by a massless, extensible tether with longitudinal damping. We refer to Beletsky and Levin[1] for the following differential equations of the tether system.

$$\begin{pmatrix} \ddot{x} - 2\dot{y}\omega - \dot{\omega}y - (1+2\kappa^{-1})\omega^2 x \\ \ddot{y} + 2\dot{x}\omega + \dot{\omega}x - (1-\kappa^{-1})\omega^2 y \\ \ddot{z} + \kappa^{-1}\omega^2 z \end{pmatrix} = \frac{1}{m_A}\begin{pmatrix} T_x + F_x \\ T_y + F_y \\ T_z + F_z \end{pmatrix}, \tag{5}$$

where the stiffness term is

$$\begin{pmatrix} T_x \\ T_y \\ T_z \end{pmatrix} = -\frac{E}{r}(\frac{r}{l} - 1)\begin{pmatrix} x \\ y \\ z \end{pmatrix},$$

$\kappa = 1 + e\cos f$, ω is the angular velocity of the center of mass, r is the distance from the center of mass to the end mass, E is called the extensional stiffness, l is the unconstrained length from the center of mass to the end mass, e is the orbital eccentricity, and f is the true anomaly. Let us be careful to interpret these equations correctly. In [1] the equations are referenced to some massive object at one end point producing a center of mass at that end point. These equations are still valid when the center of mass is somewhere in the middle of the two object as for TiPS.

Let us be precise about what exactly is modeled in these equations. Within the left side is the difference in the Keplerian forcing term $-\mu\mathbf{r}/r^3$ evaluated at the center of mass, and the end mass. The residual forcing terms on the right could include forces like higher order gravitational harmonics, drag, solar radiation pressure, and relativistic forces. However, in all cases the forces in the tether equations are the differences between the force acting on the end mass, and the force acting at the center of mass. Because the tether for TiPS is only 4 km long, these force differences are extremely small and thus will be neglected. However, there is the accumulated gravity gradient tension along the tether that is accounted for in the vector function $\mathbf{T}$. We include in the model an internal viscous damping term caused by the friction of the tether fibers.

A tethered system has a pendulum like motion, therefore, it is often convenient to consider the motion in spherical coordinates. Thus the state vector in spherical coordinates for the tether system is given by

$$\mathbf{X}_T = \mathrm{col}(\theta, \dot{\theta}, \phi, \dot{\phi}, r, \dot{r}).$$

The angles are illustrated in Figure 5. Relating them to (x, y, z) we have

$$x = r\cos\phi\cos\theta, \quad y = r\cos\phi\sin\theta, \quad z = r\sin\phi.$$

The Cartesian differential equations can easily be converted to spherical coordinates by applying the matrix

$$A = \begin{pmatrix} -\sin\theta & \cos\theta & 0 \\ -\cos\theta\sin\phi & -\sin\theta\sin\phi & \cos\phi \\ \cos\theta\cos\phi & \sin\theta\cos\phi & \sin\phi \end{pmatrix},$$

to the differential equations. The spherical equations become

$$\begin{aligned}
\ddot{\theta} + \dot{\omega} + (\dot{\theta} + \omega)\left(\frac{2\dot{r}}{r} - 2\dot{\phi}\tan\phi\right) + \frac{3\omega^2}{\kappa}\sin\theta\cos\theta &= \frac{F_\theta}{mr\cos\phi} \\
\ddot{\phi} + \frac{2\dot{r}}{r}\dot{\phi} + \left((\dot{\theta} + \omega)^2 + \frac{3\omega^2}{\kappa}\cos^2\theta\right)\sin\phi\cos\phi &= \frac{F_\phi}{mr} \\
\ddot{r} - r\left(\dot{\phi}^2 + (\dot{\theta} + \omega)^2\cos^2\phi + \frac{\omega^2}{\kappa}(3\cos^2\phi\cos^2\theta - 1)\right) &= -\frac{T}{m} + \frac{F_r}{m}.
\end{aligned} \tag{6}$$

The relation between the Cartesian and spherical force terms is given by

$$\begin{pmatrix} F_r \\ F_\theta \\ F_\phi \end{pmatrix} = A \begin{pmatrix} F_x \\ F_y \\ F_z \end{pmatrix}. \tag{7}$$

We make a few comments that we think are important. The spherical equations are more intuitive than the Cartesian form. As we will see presently, certain forces like damping are more easily expressed in spherical coordinates. In constructing the spherical form of the equations one sees that a division by $\cos\phi$ was made. This makes the equations invalid for ϕ close to $\pi/2$. While the system is expected to be more or less nadir pointing we still did not want to have a nonessential singularity in the equations. However, this does not make the Cartesian form of the equations applicable to large angles because the tether could go slack in those instances and the equations would be invalid.

4.5 Damping

The radial displacement can be expected to experience a certain amount of damping due to the tether fibers rubbing on each other and other factors. Thus we introduce into our equations a longitudinal damping term $c\dot{r}$ proportional to the radial velocity of the tether. This is easily introduced in the spherical equations (6) by

$$F_r = -c\dot{r},$$

where we would want c to be some small positive quantity. The damping is expected to be 1-2% of critical damping. We will attempt to estimate the damping parameter c. If we invert the A matrix we get the Cartesian forcing terms,

$$\begin{pmatrix} F_x \\ F_y \\ F_z \end{pmatrix} = A^{-1} \begin{pmatrix} F_r \\ F_\theta \\ F_\phi \end{pmatrix} = \begin{pmatrix} -c\dot{r}x/r \\ -c\dot{r}y/r \\ -c\dot{r}z/r \end{pmatrix}. \tag{8}$$

Notice that $A^{-1} = A^T$, the transpose of A.

This constitutes the complete picture of the equations of motion that we will work with for this paper.

4.6 Variational State Matrix

We now discuss how the $\hat{A}$ matrix of partial derivatives is determined. As was mentioned previously, this matrix is determined by integrating the variational equation (4). We need only be concerned with forming the partial derivative matrix of the forcing function $\mathbf{F}$.

The first entry in equation (4) is

$$\frac{\partial \mathbf{F}_{CM}}{\partial \mathbf{X}_{CM}}.$$

This term is the same as for any orbiting object, and thus will not be addressed here.

Rewritting Eq. (5) as a first order system, we get

$$\frac{d}{dt}\begin{pmatrix} x \\ \dot{x} \\ y \\ \dot{y} \\ z \\ \dot{z} \end{pmatrix} = \begin{pmatrix} \dot{x} \\ -(-2\dot{y}\omega - \dot{\omega}y - (1+2\kappa^{-1})\omega^2 x) + T_x/m_a + F_x/m_a \\ \dot{y} \\ -(2\dot{x}\omega + \dot{\omega}x - (1-\kappa^{-1})\omega^2 y) + T_x/m_a + F_y/m_a \\ \dot{z} \\ -\kappa^{-1}\omega^2 z + T_z/m_a + F_z/m_a \end{pmatrix} \tag{9}$$

The right side of equation (9) was previously referred to as the function $\mathbf{F}_T$.

4.6.1 $\dfrac{\partial \mathbf{F}_T}{\partial \mathbf{X}_{CM}}$

The term

$$\frac{\partial \mathbf{F}_T}{\partial \mathbf{X}_{CM}}$$

involves differentiating the angular velocity ω, $\dot{\omega}$, and κ with respect to the orbital initial conditions. For the developments in this section only, let us avoid a blizzard of subscripts by letting $\mathbf{X}_{CM} = col(x, y, z, \dot{x}, \dot{y}, \dot{z})$.

First we introduce the canonical polar variables[2] $(r, \theta, h, R, \Theta, H)$, where r is the radial distance, θ is the argument of latitude, h is the right ascension of the node, R is the radial velocity, Θ is the angular momentum, and H is the polar component of the angular momentum. The relation to the Cartesian coordinates and Cartesian velocities is

$$\begin{aligned} x &= r(\cos\theta\cos h - \sin\theta\cos I\sin h), \\ y &= r(\cos\theta\sin h + \sin\theta\cos I\cos h), \\ z &= r\sin\theta\sin I, \\ \dot{x} &= \frac{\Theta}{r}(-\sin\theta\cos h - \cos\theta\cos I\sin h) + \frac{R}{r}x, \\ \dot{y} &= \frac{\Theta}{r}(-\sin\theta\sin h + \cos\theta\cos I\cos h) + \frac{R}{r}y, \\ \dot{z} &= \frac{\Theta}{r}\cos\theta\sin I + \frac{R}{r}z. \end{aligned} \tag{10}$$

Then we get

$$\kappa = 1 + e\cos f, \quad \omega = \frac{d\theta}{dt} = \frac{\Theta}{r^2}, \quad \dot{\omega} = \frac{d^2\theta}{dt^2} = -\frac{2}{r}\frac{\Theta}{r^2}R.$$

We can use the fact that the transformation from Cartesian variables to the polar variables is canonical, and that Poisson brackets, defined by $(\_;\_)$, are invariant with respect to canonical transformations. It is then easy to construct

$$\frac{\partial\Theta}{\partial x} = \left(\Theta;\dot{x}\right)_{\text{Cartesian}} = \left(\Theta;\dot{x}\right)_{\text{polar}} = -\frac{\partial\dot{x}}{\partial\theta}.$$

Similar constructions produce the following partial derivatives for Θ,

$$\begin{aligned} \frac{\partial\Theta}{\partial x} &= -\frac{\partial\dot{x}}{\partial\theta}, & \frac{\partial\Theta}{\partial y} &= -\frac{\partial\dot{y}}{\partial\theta}, & \frac{\partial\Theta}{\partial z} &= -\frac{\partial\dot{z}}{\partial\theta}, \\ \frac{\partial\Theta}{\partial\dot{x}} &= \frac{\partial x}{\partial\theta}, & \frac{\partial\Theta}{\partial\dot{y}} &= \frac{\partial y}{\partial\theta}, & \frac{\partial\Theta}{\partial\dot{z}} &= \frac{\partial z}{\partial\theta}. \end{aligned}$$

The partials for R are

$$\begin{aligned}
\frac{\partial R}{\partial x} &= -\frac{\partial \dot{x}}{\partial r}, & \frac{\partial R}{\partial y} &= -\frac{\partial \dot{y}}{\partial r}, & \frac{\partial R}{\partial z} &= -\frac{\partial \dot{z}}{\partial r}, \\
\frac{\partial R}{\partial \dot{x}} &= \frac{\partial x}{\partial r}, & \frac{\partial R}{\partial \dot{y}} &= \frac{\partial y}{\partial r}, & \frac{\partial R}{\partial \dot{z}} &= \frac{\partial z}{\partial r}.
\end{aligned}$$

The partials of r are more straight forward,

$$\begin{aligned}
\frac{\partial r}{\partial x} &= \frac{x}{r}, & \frac{\partial r}{\partial y} &= \frac{y}{r}, & \frac{\partial r}{\partial z} &= \frac{z}{r}, \\
\frac{\partial r}{\partial \dot{x}} &= 0, & \frac{\partial r}{\partial \dot{y}} &= 0, & \frac{\partial r}{\partial \dot{z}} &= 0.
\end{aligned}$$

We now have the partials of the orbital quantities in equation (5) with respect to the orbital Cartesian coordinates given by

$$\begin{aligned}
dw &= \omega\left(\frac{d\Theta}{\Theta} - \frac{2dr}{r}\right) \\
d\dot{\omega} &= \dot{\omega}\left(\frac{d\Theta}{\Theta} + \frac{dR}{R} - \frac{3}{r}dr\right) \\
d\kappa &= \kappa\left(\frac{2d\Theta}{\Theta} - \frac{dr}{r}\right).
\end{aligned}$$

We will derive in detail one of the partial derivatives in $\partial \mathbf{F}_T / \partial \mathbf{X}_{CM}$. The others can be derived similarly. Selecting F_{T2} we get the partial derivatives

$$\begin{aligned}
\frac{\partial F_{T2}}{\partial x} &= \frac{\partial F_{T2}}{\partial \omega}\frac{\partial \omega}{\partial x} + \frac{\partial F_{T2}}{\partial \dot{\omega}}\frac{\partial \dot{\omega}}{\partial x} + \frac{\partial F_{T2}}{\partial \kappa}\frac{\partial \kappa}{\partial x} \\
&= 2(\dot{y}_T + (1 + 2\kappa^{-1})\omega x_T)\frac{\partial \omega}{\partial x} + y\frac{\partial \dot{\omega}}{\partial x} - 2\kappa^{-2}\omega^2 x_T \frac{\partial \kappa}{\partial x}. \qquad (11)
\end{aligned}$$

Notice we have now put the subscript T on the variables that are the coordinates of the tether end mass in the rotating coordinate system.

4.6.2 $\dfrac{\partial F_T}{\partial \mathbf{X}_T}$

The partials of F_T with respect to the tether state vector are easy to compute. We explicitly provide one of them,

$$\begin{aligned}
\frac{\partial \mathbf{F}_{T2}}{\partial x} &= \left(1 + \frac{2}{k}\right)\omega^2 - \frac{E}{m}\left(\frac{1}{l} - \frac{1}{r} + \frac{x^2}{r^3}\right) + \frac{\partial F_x}{\partial x}, \\
\frac{\partial \mathbf{F}_{T2}}{\partial \dot{x}} &= \frac{\partial F_x}{\partial \dot{x}}, \\
\frac{\partial \mathbf{F}_{T2}}{\partial y} &= \dot{\omega} - \frac{E}{m}\frac{xy}{r^3} + \frac{\partial F_x}{\partial y}, \\
\frac{\partial \mathbf{F}_{T2}}{\partial \dot{y}} &= 2\omega + \frac{\partial F_x}{\partial \dot{y}} \\
\frac{\partial \mathbf{F}_{T2}}{\partial z} &= -\frac{E}{m}\frac{xz}{r^3} + \frac{\partial F_x}{\partial z}, \\
\frac{\partial \mathbf{F}_{T2}}{\partial \dot{z}} &= \frac{\partial F_x}{\partial \dot{z}}.
\end{aligned}$$

Be aware that we have shifted our notation back to using $(x, y, z, \dot{x}, \dot{y}, \dot{z})$ for the Cartesian coordinates of the tether end mass.

The partials of the damping function, F_x, are

$$\begin{aligned}
\frac{\partial F_x}{\partial x} &= -\left(\frac{c\,(2x\dot{x}+y\dot{y}+z\dot{z})}{r^2} - \frac{2x^2c\,(x\dot{x}+y\dot{y}+z\dot{z})}{r^4}\right)\\
\frac{\partial F_x}{\partial \dot{x}} &= -\frac{x^2c}{r^2}\\
\frac{\partial F_x}{\partial y} &= -xc\frac{\dot{y}\left(x^2+y^2+z^2\right) - 2y\,(x\dot{x}+y\dot{y}+z\dot{z})}{r^4}\\
\frac{\partial F_x}{\partial \dot{y}} &= -\frac{xyc}{r^2}\\
\frac{\partial F_x}{\partial z} &= -xc\frac{\dot{z}\left(x^2+y^2+z^2\right) - 2z\,(x\dot{x}+y\dot{y}+z\dot{z})}{r^4}\\
\frac{\partial F_x}{\partial \dot{z}} &= -\frac{xzc}{r}.
\end{aligned}$$

4.7 Simplifications

Currently we plan to numerically integrate the partial derivatives, $\hat{A}$. However, analytic partials could significantly reduce the computation time. For this reason and to obtain insight into the tether dynamics it is worthwhile to consider several simplified versions of the equations. We start with the spherical form for the tether equations, Eq. (6). Assume the system is in a near circular orbit and neglect the coupling between r, θ and ϕ. With these assumptions Eq. (6) become

$$\begin{aligned}
\ddot{\theta} + \frac{3}{2}\omega^2\sin(2\theta) &= 0,\\
\ddot{\phi} + 2\omega^2\sin(2\phi) &= 0,\\
\ddot{r} + c\dot{r} + \left(\frac{E}{m_a l} - 3\omega^2\right) r &= \frac{E}{m_a}.
\end{aligned} \tag{12}$$

The first two of Eq. (12) can be solved in terms of elliptic functions and the third is a damped harmonic oscillator. For small θ and ϕ, Eq. (12) become

$$\begin{aligned}
\ddot{\theta} + 3\omega^2\theta &= 0,\\
\ddot{\phi} + 4\omega^2\phi &= 0.
\end{aligned} \tag{13}$$

which are the equations of motion of harmonic oscillators. The frequencies of these oscillations are $\sqrt{3}\omega$ and 2ω, respectively. For TiPS the periods of the intrack and crosstrack oscillations would be approximately 60 and 52 minutes respectively. The problem is that large oscillation amplitudes are expected and the period of the oscillations is a function of the amplitude. Over a few orbits, convergence of the least squares process could be difficult. Thus, a better estimate of the oscillation period is needed. A solution can be formulated as a complete elliptic integral of the third kind. The basic equation is

$$\ddot{\beta} + \frac{b}{2}\omega^2\sin 2\beta = 0, \tag{14}$$

where b = 3, for θ and b = 4, for ϕ. Multiplying equation (14) by $\dot{\beta}$ and integrating we get

$$\dot{\beta}^2 - \frac{b\omega^2}{2}\cos 2\beta = \text{const}$$

Substituting $\cos 2\beta = 1 - 2\sin^2\beta$ we get

$$\dot{\beta}^2 + b\omega^2 \sin^2\beta = E,$$

where E is a constant. If we let β_m be the maximum value for β which occurs when $\dot{\beta} = 0$, then $E = b\omega^2 \sin^2\beta_m$. Integrating over a fourth of the period we get

$$T = 4\int_0^{\beta_m} \frac{d\beta}{E - b\omega^2 \sin^2\beta}.$$

Substituting $\sin\alpha = \sin\beta/\sin\beta_m$ we get

$$T = \frac{4}{\omega\sqrt{b}} \int_0^{\pi/2} \frac{d\alpha}{1 - k\sin^2\phi}, \quad k = \sin^2\beta_m.$$

The solution then becomes

$$T = \frac{4}{\omega\sqrt{b}} K(k),$$

where K is the elliptic integral of the third kind. The elliptic integral can be expanded in a series of the modulus k by

$$K(k) = \frac{\pi}{2}\left(1 + (\frac{1}{2})^2 k + (\frac{1\cdot 3}{2\cdot 4})^2 k^2 + (\frac{1\cdot 3\cdot 5}{2\cdot 4\cdot 6})^3 k^3 + \ldots.\right)$$

θ (deg)	ϕ (deg)	θ period coupled eqs. (min)	ϕ period coupled eqs. (min)	θ period elliptic int (min)	ϕ period elliptic int (min)
5	5	60:39-61:42	52:40-53:07	61:09	52:58
45	0	71:54-72:00	N/A	72:02	52:52
0	45	59:51-71:11	57:48-58:34	61:02	62:23
45	45	70:31-73:01	56:26-66:31	72:02	62:23
75	0	103:47-110:56	N/A	100:47	52:52
0	75	80:09-Pinwheel	59:07-94:05	61:02	87:17
75	75	82:57-Pinwheel	56:02-107:14	100:47	87:17

Table 1: Frequencies of Oscillations.

We have used the elliptic integral solution to modify the frequencies one gets for Eq. (13). The simplifications of (5) produced the decoupled Eq. (12), which, for the angles, is a system of two harmonic oscillators with different frequencies. The coupling in Eq. (5) results in the tether oscillations being nonperiodic. In Table 1 we provide some periods for the uncoupled system and ranges on the elapsed time for the angles to oscillate from peak to peak for the coupled equations. We will call the peak to peak elapsed time the period of oscillation even though the coupled system is not periodic. As can be seen the periods for the coupled system can vary by several minutes. Not accounting for this variation could affect the convergence of the orbit determination, especially when processing data over a couple of days. For this reason, we feel the uncoupled linear solutions are inadequate for anything but small oscillations about nadir. Since we expect TiPS to have oscillations with large amplitude, we have developed our system with the coupled Eq. (5).

5 Software Development

The orbit determination algorithms described previously have been implemented in a Fortran program. The integrator is a 4/5 Runge-Kutta technique. The orbit equations incorporate geopotential

forces and several different drag models. We have implemented the Cartesian equations given by Eq. (9) and partial derivatives as discussed in Section 4.6.

We have also developed a program that implements the analytic solutions for Eq. (12) with the frequency estimation discussed in Section 4.7. For the partials we programmed the partial derivatives of the analytic solution.

Limited validation of these programs has been performed at this time. The programs will differentially correct initial conditions using simulated tether data as long as the starter initial conditions are not too far off the true initial conditions. The process we go through is to generate tether orbital data by applying one of the tether models to the initial conditions for the tether state vector. Then we feed corrupted initial conditions to the differential correction program. As long as the corrupted initial conditions are not too far from the truth, the differential correction will converge to the true initial conditions. However the differential correction system is very sensitive to the starter initial state. For small amplitudes in the angles one can normally start with a tether state of zero for all tether angles and angular rates. As one progresses up to tether initial conditions corresponding to 50^o in intrack and crosstrack angles the starter initial conditions cannot be more than a few degrees off of the maximum amplitude. This is not surprising since large angles in tether oscillations could produce observations that appear to be intrack or crosstrack orbital variations and could serve to "confuse" the center of mass part of the orbit determination.

True IC				A Priori Estimate			
Orbit		Tether		Orbit		Tether	
a:	7401.36	θ:	20.0	a:	7400.40	θ:	16.0
e:	0.000626	$\dot{\theta}$:	0.0	e:	0.000607	$\dot{\theta}$:	0.0
i:	63.435	ϕ:	20.0	i:	63.442	ϕ:	16.0
f:	-140.095	$\dot{\phi}$:	0.0	f:	-153.763	$\dot{\phi}$:	0.0
ω:	0.049	r:	3.0002	ω:	13.729	r:	3.1000
Ω:	90.000	$\dot{r}$:	0.0	Ω:	89.991	$\dot{r}$:	0.0

Table 2: Initial Conditions for Tether Orbit Determination.

We provide in Tables 2 and 3 the initial conditions and results from one differential correction with the system. Angles and angular rates are in degrees and degrees/sec, distances are in kilometers and velocities are in kilometers/second. For the orbit determination the tether initial conditions were held fixed for four iterations in order to allow the center of mass to converge without corrupting the first estimate of the tether initial conditions. Otherwise the program is unable to converge to the correct initial conditions for the full system. A data set spanning 24 hours was used for this run, with the data distributed at 60 second intervals. The equations for the predictor and the orbit determination used the coupled equations in Eq. (5) and the partial derivatives described in Section 4.6.

We are now proceeding to embed the tether equations and partial derivatives into a standard orbit determination system called GEODYN which will be used for the operational system.

6 Analysis

We expect to have a reasonably good estimate of the orbit after jettison. Separation occurs 175 minutes after jettison and the first pass over a tracking station should occur within several orbits. Although we will have some knowledge of the attitude of TiPS at the time of separation, our knowledge of the initial state of the deployed system will be based on a crude deployment simulation. Thus, our initial tether state will not be very good, although we will have a good estimate of the orbit of the center of mass. Therefore, two key questions which must be answered are:

- What is the range of convergence of the DC for the tether system attitude?

Iteration	RMS (m)	X (km)	Y (km)	Z (km)	θ (deg)	ϕ (deg)	r (km)
0	69876.0	2125.6	-5675.3	-4254.2	16.0	16.0	3.10
1	15845.6	2123.1	-5681.7	-4246.9	16.0	16.0	3.10
2	1129.3	2126.1	-5677.1	-4252.3	16.0	16.0	3.10
3	1011.0	2126.6	-5676.3	-4253.3	16.0	16.0	3.10
4	921.3	2126.6	-5676.3	-4253.2	16.0	16.0	3.10
5	335.3	2126.6	-5676.3	-4253.2	16.0	17.6	3.00
6	1022.3	2126.6	-5676.3	-4253.2	22.4	21.5	3.02
7	482.6	2126.6	-5676.3	-4253.2	21.6	20.5	3.00
8	117.3	2126.6	-5676.3	-4253.2	20.1	20.2	3.00
9	21.6	2126.6	-5676.3	-4253.2	20.1	20.0	3.00
10	0.3	2126.6	-5676.3	-4253.2	20.0	20.0	3.00
11	0.0	2126.6	-5676.3	-4253.2	20.0	20.0	3.00

Table 3: Convergence to a Solution.

- Is an algorithm needed to give an estimate of the tether state so that the DC will converge?

A pointing (Extended Inter-Range) vector will be supplied by NRL to the laser tracking sites. Some of the sites have a search capability, while others do not. The SLR sites are given in Table 4. For those sites that have a search capability it is desirable that the end mass be in the laser footprint. For those sites without search capability to obtain tracking data, the end mass must be in the footprint. At the expected range of the tether, this footprint is several hundred meters. Thus we need to know

- What is the prediction time for which the end mass will be within the SLR footprint or for how long is the EIRV valid?
- How many passes are needed to converge on an EIRV with sufficient accuracy to provide pointing for future passes?

Other questions which need to be answered are:

- What is the maximum allowable fit span for the DC?
- Do we need to and will we be able to estimate the tether damping?

The analysis is focused on answering these questions. The results to date are discussed below.

Table 5 shows the range of convergence of the DC as a function of the pitch (θ) and roll (ϕ) libration amplitude. Truth was generated using an orbit propagator and the coupled differential equations, Eqs. (5), for the tether with the initial state in the column "True IC". The attitude rates, $\dot{\theta}$ and $\dot{\phi}$, were zero. A ten minute pass for a site was assumed with range, azimuth and elevation data generated every fifteen seconds. Perfect observations were used. The initial state estimate for the CM orbit was corrupted from the truth and the initial estimates for the pitch and roll amplitude were varied to determine the range of convergence. The limit of the range of convergence is given in the column "A Priori Estimate". We see that the range of convergence is 10-15 degrees except at very large libration amplitudes. From these results we conclude that an algorithm for providing an initial estimate of the tether attitude state is needed for the DC. An algorithm equivalent to the Herrick-Gibbs for initial orbit determination is needed.

7 Summary

For normal satellites, the motion of the center of mass is decoupled from the attitude motion, and the orbit and attitude determination can be performed independently because the observations can

Station	Organization	Min Elevation Angle (deg)
Haleakala	NASA	20
Easter Island	NASA	20
Quincy	NASA	20
Monument Peak	NASA	20
Starfire Optical Range	DoD	30
McDonald Observatory	NASA	20
Greenbelt	NASA	30
Arequipa	NASA	20
Yarragadee	NASA	20
Herstmonceaux	EUROLAS	20
Grasse	EUROLAS	20
Wettzell	EUROLAS	20
Graz	EUROLAS	20
Orroral	Pacific	20

Table 4: Average SLR Coverage

True IC		A Priori Estimate	
θ	ϕ	θ	ϕ
10	10	0	0
15	15	5	5
25	25	10	10
35	35	15	15
45	45	25	25
50	50	40	40
55	55	48	48
60	60	56	56

Table 5: One Pass Range of Convergence. Observations generated without noise.

be considered to be of the center of mass. In contrast, for a tethered satellite system when one or both subsatellites are tracked, the observations are affected by the attitude motion of the tether system. Therefore, the orbit determination of the center of mass of the tether system cannot be decoupled from the attitude determination of the system. In this paper the method for the orbit and attitude determination of TiPS has been described.

The tether has been assumed to be massless and extensible with viscous damping. The motion of the tether system is described by the motion of the center of mass (CM) of the system and the motion of the end masses relative to the CM in a local vertical, local horizontal coordinate system. The equations of motion and the variational equations are numerically integrated. Analytic partials for the attitude motion have also been developed and evaluations on their use are planned. Since numerical integration is used there are no restrictions on the orbit model. In this study a 4 x 4 geopotential model with a MSISE drag model was used.

Conclusions to date are:

- The range of convergence for the libration amplitude in the differential correction (DC) is 10-15 degrees except for very large libration amplitudes.
- An algorithm for providing an initial estimate of the libration amplitude and rates is needed for the DC to ensure that the initial estimate is within the 10-15 degree maximum libration amplitude.

8 Acknowledgments

We acknowledge the help of Mr. Robert Towsley and Mr. Bill Purdy, the TiPS project managers, for their contributions to our understanding of the TiPS mission, and the help of Mr. Gary Shu, Allied Signal Corporation, for the engineering drawings of TiPS. Stuart Morgan provided help in debugging the DC software.

Authors are listed in alphabetical order.

References

[1] Beletsky, V. V. and Levin, E. M., Dynamics of Space Tether Systems, Advances in the Astronautical Sciences, Vol. 83, 1993.

[2] Deprit, A.: "The Elimination of the Parallax in Satellite Theory," *Celestial Mechanics* **24**, 111-153.

[3] "Small, Expendable Tether Deployer Systems Analysis of SEDS-1 Flight Results," NASA Report 057.0494.TR.